This is the pre-peer reviewed version of the following article

Pedro J. Silva and Maria J. Ramos (2011) "Computational insights into the photochemical step of the reaction catalyzed by protochlorophylide oxidoreductase". which has been puclished in final format in *Int. J. Quantum Chem.*,111, 1472-1479

Computational insights into the photochemical step of the reaction catalyzed by protochlorophylide oxidoreductase

Pedro J. Silva[§] *and Maria João Ramos*[†*]

[§]Fac. de Ciências da Saúde, Univ. Fernando Pessoa, Rua Carlos da Maia, 296, 4200-150 Porto-Portugal

[†]REQUIMTE, Faculdade de Ciências do Porto, Rua do Campo Alegre, 687, 4169-007 Porto – Portugal

Abstract:

The light-dependent enzyme protochlorophyllide oxidoreductase (PChOR) (EC:1.3.1.33) catalyzes the conversion of protochlorophyllide into chlorophyllide, during chlorophyll synthesis. The reaction has been proposed to proceed through light-induced weakening of the C17-C18 double bond in protochlorophyllide, which then facilitates hydride transfer from a NADPH co-substrate molecule. We have performed DFT and TDDFT computations on the reaction mechanism of this interesting enzyme. The results show that whereas in the ground state the reaction is strongly endergonic and has a very high activation free energy (38 kcal.mol-1), the first four excited states (corresponding to excitations within the conjugated porphyrin π-system) afford much lower activation free energies (<25 kcal.mol-1) and spontaneous (or only slightly endergonic) reaction paths. The sharp shape of the potential energy surface along the reaction coordinate in these excited states allows hydrogen tunneling to occur efficiently on the first excited state surface, lowering the barrier to values closer to experiment, in agreement with recent suggestions.

*corresponding author: mjramos@fc.up.pt

I. Introduction

Chlorophyll is by far the most abundant biological pigment in Nature. Due to its role harvesting sunlight in photosynthesis, it is ultimately responsible for the fixation of almost all free energy available to biological systems. In vivo, chlorophyll is synthesized from protoporphyrin IX in a pathway[1] that leads (through sequential Mg insertion, methylation and a six-electron oxidation) to protochlorophyllide (PChlide). Stereospecific reduction of the PChlide D ring followed by esterification with a long-chain polyisoprenol then yields chlorophyll. The reduction of the protochlorophyllide D ring may be catalyzed by two different-enzymes: angiosperms contain a light-dependent PChlide oxidoreductase (EC 1.3.1.33) which uses NADPH as electron donor, whereas other plants, algae and cyanobacteria also contain a light-independent PChlide oxidoreductase (EC 1.18.-.-)[2].

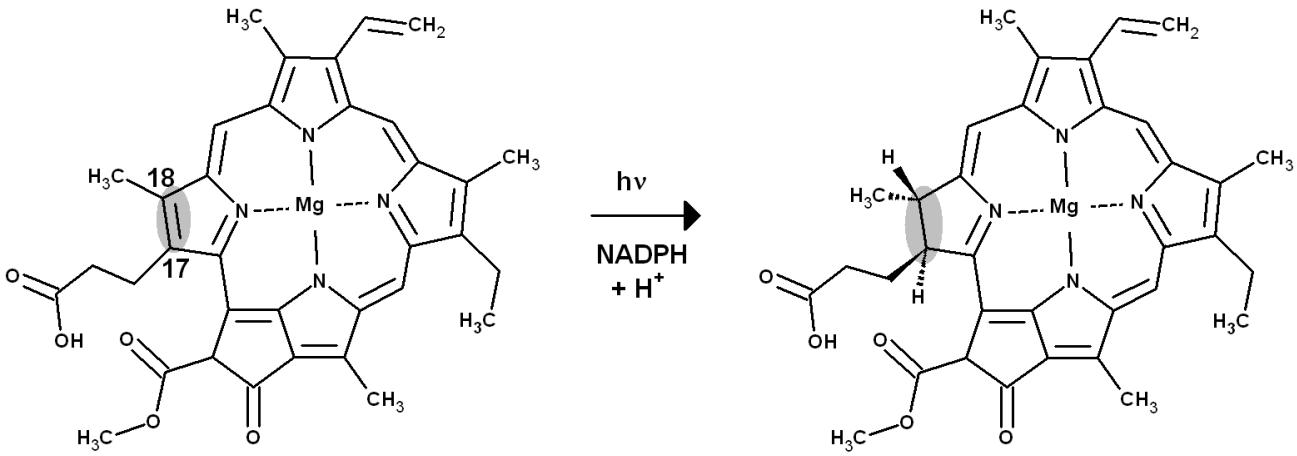

Fig. 1: The reaction catalyzed by the light-dependent protochlorophyllide oxidoreductase.

Upon illumination, the light-dependent NADPH:protochlorophyllide oxidoreductase catalyzes the transfer of hydride from the pro-S face of NADPH[3,4] to the C17 atom of the D-ring of PChlide, followed by proton transfer from a conserved tyrosine residue to the C18 atom of this ring (Figure 1). A conserved lysine residue in close proximity to this tyrosine is believed to stabilize the negative charge formed on the tyrosine phenol ring, thereby facilitating the proton transfer[5]. Detailed kinetic analyses of

the reaction at low temperatures have shown the reaction to consist of an initial light-driven step (which yields a charge-transfer complex[6]) followed by several light-independent steps (corresponding to proton transfer from the enzyme to the charge-transfer complex and to a series of ordered product release and cofactor binding events[7,8,9]). In spite of these extensive investigations, the precise mechanism of the light-dependent step remains poorly understood. Recently, Heyes *et al.* described unusual kinetic isotopic effects in the reaction mechanism[10], characteristic of quantum tunneling of hydrogen nuclei in the reaction mechanism, and characterized its ground-state potential energy surface through density-functional computations.

In this report, we describe additional quantum-mechanical computations on the ground- and excited-state potential energy surfaces of the (light-dependent) hydride transfer step of this interesting enzyme. The results show that whereas in the ground state the reaction is strongly endergonic and has a very high activation free energy (38 kcal.mol-1), the first excited states (corresponding to excitations within the conjugated porphyrin π-system) afford much lower activation free energies (<25 kcal.mol-1) and spontaneous (or only slightly endergonic) reaction paths. We also computed the probability of quantum tunneling of hydrogen nuclei along the reaction coordinate in these low-lying excited states, and show that hydrogen tunneling may occur efficiently on the first few excited potential energy surfaces, lowering the barriers to values closer to experiment.

II. Computational Methods

All calculations were performed at the B3LYP level of theory[11,12,13]. Autogenerated delocalized coordinates[14] were used for geometry optimizations, using a medium-sized basis set, 6-31G(d), since it is well known that larger basis sets give very small additional corrections to the geometries, and their use for this end is hence considered unnecessary from a computational point of view[15,16,17]. The model system included 113 atoms: a protochlorophyllide molecule (with the ethyl substituent on the ring substituted by methyl), NADPH (modeled as nicotinamide) and three water molecules on each side of

the porphyrin plane (in order to simulate solvation effects and complete the Mg coordination sphere). Unfortunately, no active site amino acids could be included in our model for two related reasons: (i) although a tentative homology model of PChoR is available[18], this has not been corroborated experimentally; (ii) because of the large size of the system, inclusion of uncorroborated amino acids would make the computation prohibitively expensive without ensuring unambiguously better results. Atomic charge and spin density distributions were calculated with a Mulliken population analysis[19] based on symmetrically orthogonalized orbitals[20]. All calculations were performed with the PC GAMESS/Firefly quantum chemistry package[21], which is partially based on the GAMESS (US)[22] source code. The potential energy surface for the reaction in the ground state was obtained by sequentially constraining the distance between the NADPH pro-S hydrogen and Pchlide C17 atom, and optimizing the resulting structures. Geometry optimization of excited states is prohibitively demanding in computational resources, and therefore approximate potential energy surfaces of the first thirteen excited states were obtained by performing time-dependent density functional theory computations on each of the (ground-state-optimized) scan points. Whereas most of these excited states arise from excitations within the porphyrin π-system (Fig. 4), the 3rd and 4th excited states computed by TDDFT arise from charge-transfer from NADPH to the porphyrin. Time-dependent DFT is known to fail in the analysis of excited states with important double-excitation or charge-transfer character, e.g. by not reproducing the correct dependence of the energy of a charge-separated system with the inverse of the distance between its oppositely-charged moieties[23,24,25,26], and additional computations were required to ascertain the feasibility of these excitations. We therefore computed the vertical excitation energy between the ground state reactants and the charge-transfer PChlide^{-}/NADPH^{+} system at the same theoretical level. Since the self-consistent field computation of this two-component system, however, always converged to the ground state, we computed the energy of *isolated* PChlide^{-} and NADPH^{+} vs. *isolated* PChlide and NADPH (in the presence of suitable ghost orbitals in order to account for basis set superposition errors). This infinitely separated charge-transfer system is computed to lie 129.0 kcal.mol^{-1} above the ground state in the gas-phase. The vertical separation between the neutral and charge-trasfer states at *finite*

separation may be computed from this value by applying a correction based on the CIS formalism[26], which does not suffer from the electron-transfer self-interaction observed in TDDFT. The total stabilization when bringing the oppositely-charged moieties to a 2.06 Å distance amounts to 35 kcal.mol^{-1} (3.3 kcal.mol^{-1} from taking two oppositely charged electronic point charges from infinity to within 100 Å of each other, as computed through Coulomb's law, plus 31.7 kcal.mol^{-1} excited state stabilization when taking the system from 100 Å to 2.06 Å, computed from CIS). Low-wavelength photons (≈300 nm) are still required to attain this charge-separated state (in considerable disagreement with the experimental observation of catalysis upon irradiation with 690 nm photons). These charge-transfer states were therefore excluded from our analysis.

The contribution of hydrogen tunneling to the reaction rate was computed with the well-known semiclassical approximation to the transmission probability for an energy E below the barrier height V_{max}[27,28,29,30,31], as described by Garret and Truhlar[32]. In this methodology, the variation in transmission coefficient, κ, due to quantum effects (tunneling though the barrier and reflection above the barrier) is computed as the ratio of Boltzmann-averaged quantum and classical transmission probabilities:

$$\kappa = \frac{\int_0^{\infty} T(E)\, e^{-\beta E} dE}{\int_{V_{max}}^{\infty} e^{-\beta E} dE}$$, where $\beta=1/k_B T$, k_B is Boltzmann's constant, and T(E) is the quantum transmission coefficient at energy E. For energies below the barrier, T(E) is computed from the semiclassical approximation $T(E) = \frac{1}{1+e^{2\theta(E)}}$, where the barrier penetration integral θ(E) is given by

$$\theta(E) = \frac{2\pi}{h}\int_a^b \sqrt{2\mu(V(s)-E)}\ \ ds$$, and *a* and *b* are the locations at which V(s)=E, and μ is the reduced mass of the tunneling particle. Analysis of these expressions shows that the transmission coefficient at the top of the barrier is not 1, as in the classical case, but ½, due to the possibility of quantum reflection. For energies slightly above the barrier (between V_{max} and $2\times V_{max}$) Garret and Truhlar[30] have derived an expression for T(E) assuming a parabolic potential, an approximation which yields T(E)=1 for energies

in excess of $2\times V_{max}$, and T(E) between ½ and 1 for energies between V_{max} and $2\times V_{max}$. Since a parabolic approximation is not suitable for the potential energy surfaces studied in this work, we took a conservative approach in the evaluation of transmission probabilities above the barrier: for energies slightly above the barrier (between V_{max} and $2\times V_{max}$), we set $T(E)=T(V_{max})=½$, and set T(E)=1 for energies above $2\times V_{max}$. In any case, the precise choice of values for the transmission coefficient above the barrier does not usually affect the computations (except in the case of very low barriers or very high temperatures), since Boltzman-averaging ensures that most of the quantum-mechanical contributions to the transmission coefficient arise from highly-populated (and therefore low-energy) paths.

It must be noted that the presence of hydrogen tunneling affects the reaction rate by altering the value of the transmission coefficient (κ) in the Eyring equation

$$k = \kappa \frac{k_B T}{h} e^{\frac{-\Delta H^{\ddagger}}{RT} + \frac{\Delta S^{\ddagger}}{R}}$$

, rather than the energetic barrier itself. On the other hand, estimates of the energetic barrier from experimental values of the reaction rate usually assume that the transmission coefficient equals 1. Therefore, the energetic barrier deduced from measurements of the light-dependent reaction rate of PChOR[10] (as well as its decomposition in enthalpic and entropic contributions) is an *apparent* value, and is actually a function of both the real thermodynamic barrier and the tunneling-dependent transmission coefficient.

III. Results and discussion

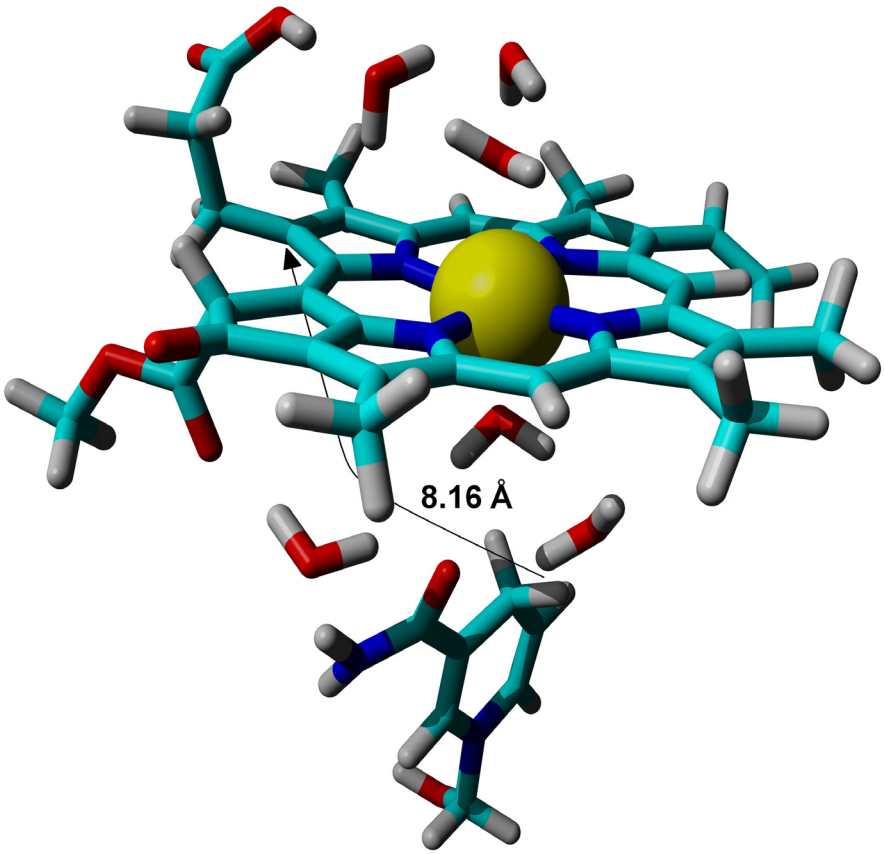

Fig. 2: Optimized structure of the reactants in the light-dependent PChOR-catalyzed reaction.

Optimization of the initial geometry of the reagents shows that in the absence of any sterical constrains NADPH adopts a perpendicular position relative to the protochlorophyllide porphyrin plane (Figure 2). In this conformation, the carbon atom bearing the reacting hydride lies 5.79 Å away from the central Mg atom, but the reacting *pro*-S hydrogen in NADPH lies quite far (8.16 Å) from the protochlorophyllide C17 atom. These structural parameters are not compatible with the active site dimensions deduced from the available homology model of light-dependent PChlide oxidoreductase[18]: according to the model, the active site constrains the relative orientation of the NADPH and PChlide, so that the reacting hydride lies ≈3.8 Å from the substrate C17 atom. On the other hand, counterpoise[33] calculations reveal that electronic interactions between NADPH and PChlide stabilize the complex by 5.5 kcal.mol^{-1} *vs.* the separated reactants. Therefore, whereas geometrical distortions of the gas-phase

structure imposed by the catalytic site yield thermodynamically "sub-optimal" structures, the electronic stabilization of the complex still provides an incentive for complex formation. For example, as the distance between the pro-S hydrogen and the C17 atom decreases to 3.96 Å the complex becomes less stable by 3.0 kcal.mol^{-1}, but its formation from the isolated reactants is still favored by 2.5 kcal.mol^{-1}. These observations, coupled with the fact that the experimental geometry of the enzyme-bound NADPH-PChlide complex has not been determined, mean that the *absolute* value of the energetic barrier between the enzyme-bound reactants and the transition state cannot be confidently computed. The *relative* differences of these energetic barriers in the ground- and the first excited-states, however, is quite insensitive to the initial geometry, since their potential energy surfaces are almost parallel from the optimized reactants to a hydrogen-carbon distance of 2.0 Å (Fig. 3).

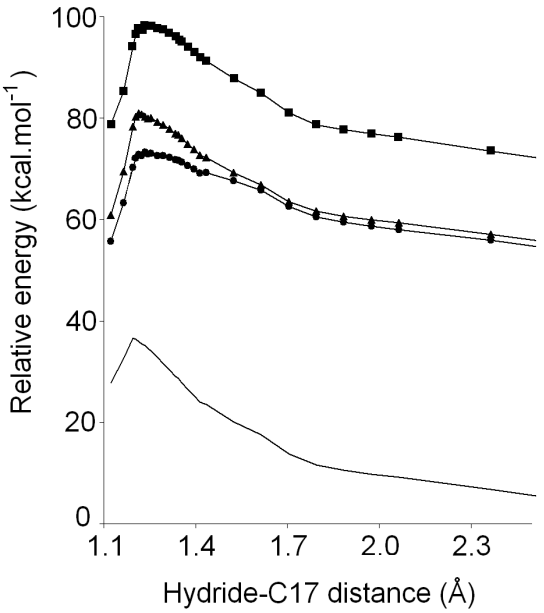

Fig. 3: Potential energy surface of the PChlide-catalyzed reaction in the ground state and selected excited states (●) 1st excited state; (▲) 2nd excited state; (■)3rd excited state. For ease of comparison with the homology modeled structure of PChOR, the relative energy scale has been zeroed at the electronic energy of the ground state at a hydride-C17 distance of 3.96 Å (which lies 3.0 kcal.mol^{-1} above the computed absolute minimum with 8.16 Å hydride-C17 distance).

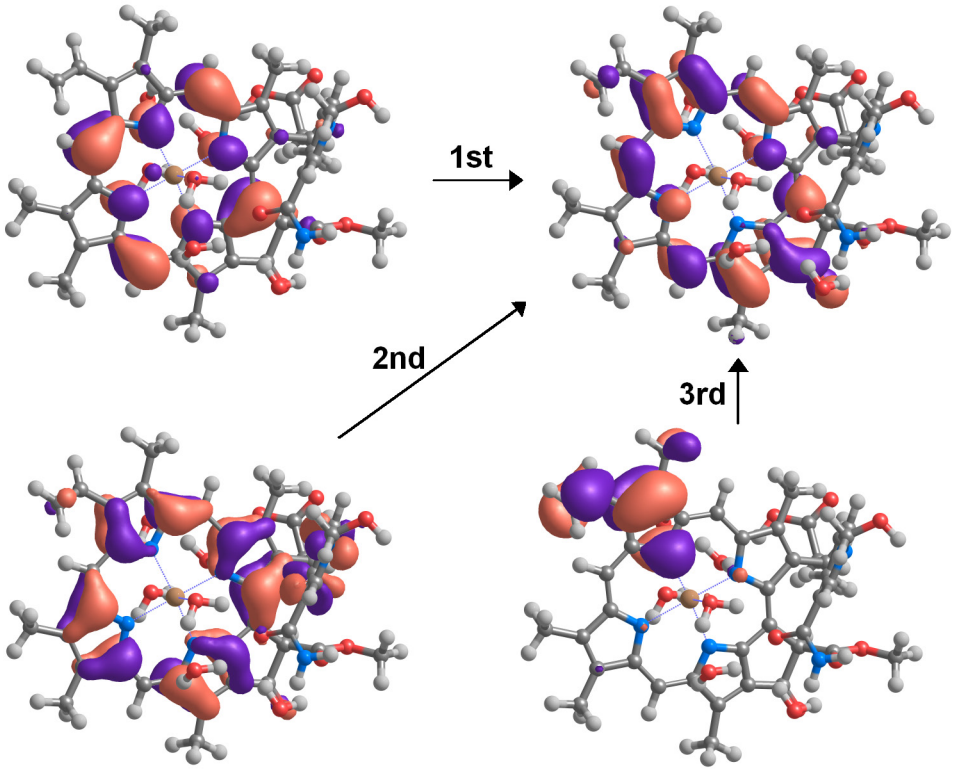

Fig. 4: Molecular orbitals involved in the transitions to the first three excited states, as computed by time-dependent DFT. As explained in the Methods section, TDDFT computations detect two additional (charge-transfer) excited states with energies between those of the 2nd and 3rd transitions shown.

For ease of comparison with the homology modeled structure of PChOR, all energies reported henceforth are measured relative to the structure bearing a hydride-C17 distance of 3.96 Å. The ground-state potential energy surface is highly endergonic (27.7 kcal.mol^{-1}) and is clearly incompatible with the fast reaction rates observed experimentally, as it yields an activation electronic energy of 36.6 kcal.mol^{-1}. *In vivo*, the reaction is expected to occur on the first excited state surface (Fig. 3), as it can be elicited by illumination of the enzyme-substrate complex with a 690 nm wavelength (which is the lower energy electronic transition of the protochlorophyllide:NADPH system). Indeed, the potential energy surfaces of the first three excited states (Fig. 3) generally afford much more favorable conditions: the reaction on the first excited surface is slightly endergonic by 6.3 kcal.mol^{-1}, and on the 2nd and 3rd excited states the reaction proceeds with moderate endergonicity between 9 and 13 kcal.mol^{-1}. Most importantly, the activation energies in these excited surfaces are remarkably lowered (by 13-14 kcal.mol^{-1} in the 1st

excited state, and 6-7 kcal.mol^{-1} in the remaining states) in regard to that of the ground state (Table 1), although they still remain above the experimentally determined activation free energies (*apparent* $\Delta G^{\ddagger}$ = 6.7 kcal.mol^{-1} at 298 K, computed from the values in ref. 10). The difference may be partially attributed to the neglect, in our computations, of vibrational contributions to the enthalpy, which are prohibitively expensive to compute as they require the very demanding computation of the matrix of second partial derivatives on geometries optimized *separately* at each ground- and excited-state. An additional factor that intervenes in lowering the activation energies has been identified by Heyes et al.[10] in measurements of the enzyme kinetic parameters with naturally occurring vs. deuterated NADPH: the very strong kinetic isotope effect measured experimentally clearly shows the involvement of quantum tunneling of hydrogen nuclei[34] from NADPH to the porphyrin substrate.

	ΔE (kcal.mol^{-1})	$\Delta E^{\ddagger}$ (kcal.mol^{-1})	Apparent $\Delta E^{\ddagger}$ (kcal.mol^{-1}) (including quantum effects)
Ground State	27.7	36.6	30.0
First excited state	6.3	23.8	18.4
Second excited state	10.3	30.3	19.9
Third excited state	11.6	31.2	21.2

Table 1: Reaction and activation energies of the PChOR reaction on the ground- and the first five excited potential energy surfaces.

Explicit inclusion of tunneling effects along the one-dimensional C17-hydride reaction coordinate lowers the *apparent* reaction barriers by another 5-10 kcal.mol^{-1} (at 298 K), depending on the individual potential energy surfaces (Table 1). The importance of hydrogen tunneling increases as the potential energy surfaces becomes sharper, as can be readily observed by comparing the shape of the surfaces with higher tunneling contributions (the 2nd and 3rd excited states) with that of the first excited state. Further, as the reaction temperature is lowered the number of molecules with energy above the

thermodynamic activation barrier decreases exponentially, so that the *relative* contribution of quantum tunneling increases dramatically. An Eyring plot of the predicted reaction rates therefore shows a spurious dependence on temperature (Fig.5), an often overlooked fact which prevents the collection of meaningful estimates of the reaction activation enthalpy and entropies from experimental reaction rates whenever tunneling (or other effects) yields temperature-dependent transmission coefficients.

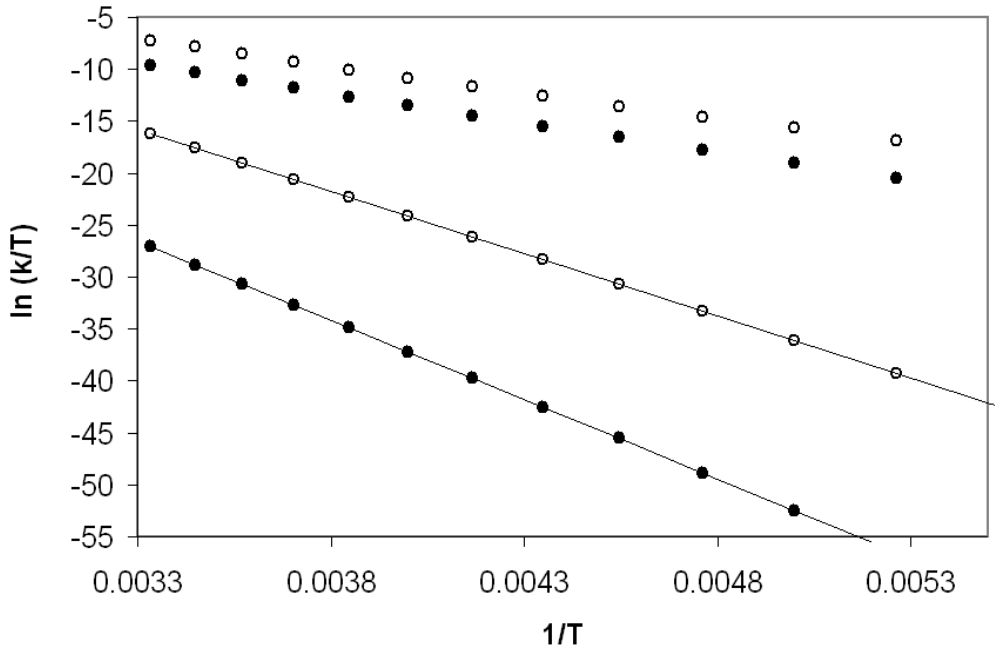

Fig. 5: Eyring plots of the computed reaction rates of hydride transfer on the (○) 1st and (●) 2nd excited potential energy surfaces, assuming constant activation barriers of 23.8 kcal.mol^{-1} (1st excited state) and 30.3 kcal.mol^{-1} (2nd excited state), either excluding (lined data) or including (scattered data) tunneling effects. In this representation, the activation ΔS and ΔH may be computed from the ordinates at the origin and slope (respectively) of the straight lines drawn from the experimental data. Inclusion of tunneling effects leads to wrong estimates of $\Delta H^{\ddagger}$ (8.8 kcal.mol^{-1} for the 1st excited state and 10.8 kcal.mol^{-1} for 2nd excited state) and $\Delta S^{\ddagger}$ (-33.6 cal.mol^{-1}.K^{-}1 for the 1st excited state and -31.0 cal.mol^{-1}.K^{-}1 for the 2nd excited state).

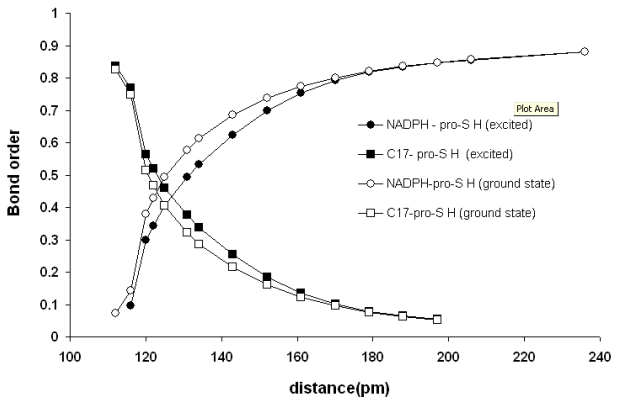

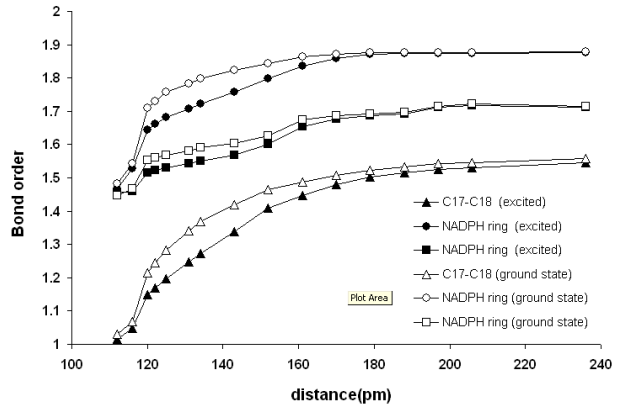

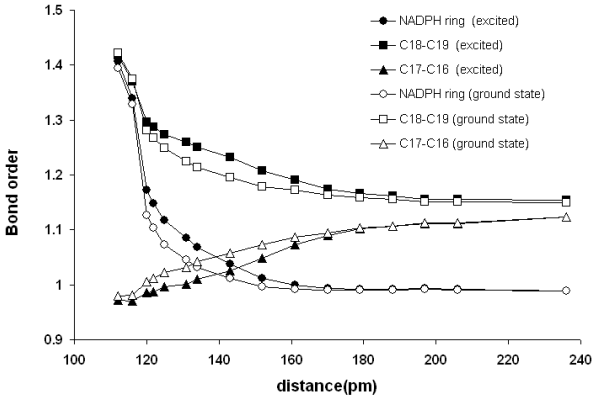

Fig. 6: Comparison of selected bond orders between the ground state and 1st excited states as NADPH approaches the PChlide.

Analysis of the charge distribution and bond orders on the porphryin and NADPH molecules on the 1st excited surface (Figure 6) reveals additional information on the subtle electronic factors favoring the reaction under these circumstances (vs. ground state): specifically, there are almost no differences in bond orders on the 1st excited (vs. ground) state as NADPH approaches the protochlorophyllide from afar. Only as the *pro*-S HADPH hydrogen moves closer than 2.0 Å from the porphyrin C17 can any

measureable differences be found (which is consistent with the constant energy separation between these two electronic states at separations above 2.0 Å): the bond between C17 and C18 then becomes weaker on the excited state, at the same time as the bond pattern on the nicotinamide ring changes from the familiar two-double/four-single bonds characteristic of NADPH to the six fully-delocalized π-electrons characteristic of $NADP^+$.

Conclusions

Although the lack of a crystal structure of the PChOR:PChlide:NADPH and the large computational cost of excited-state optimization prevented us from performing a fully detailed and realistic analysis, the simplified model we used afforded several interesting insights into the reaction mechanism of this interesting enzyme:

a) the potential energy surface on the 1st excited state (which is expected to be the most relevant state, since the reaction proceeds upon illumination of the lowest-energy absorption band) affords ≈12 $kcal.mol^{-1}$ lowering of the activation energy vs. the reaction in the ground state;

b) hydrogen tunneling decreases the activation energy (in the 1st excited state surface) by 5.4 $kcal.mol^{-1}$, which corresponds to an increase of the reaction rate by a factor of approximately 10^4

c) measurable differences between the ground and 1st excited state only arise as the C17-*pro*-S NADPH hydrogen distance becomes shorter than 2.0 Å. Dynamic factors such as ground-state protein motions may therefore play a relevant role in bringing the NADPH molecule into close proximity of the PChlide substrate, even if in their initial binding states the two molecules lie relatively far from each other.

d) the relative magnitude of hydrogen tunneling changes dramatically with temperature, which prevents the estimation of activation ΔH and ΔS in this reaction through the familiar Eyring equation.

Acknowledgments: The authors thank Prof. Richard B. Sessions (University of Bristol) for providing the coordinates of the PChOR homology model.

Supplementary Material Available: Geometries and energies of the PChlide-NADPH complex at different distances.

V. References

1. Masuda, T.; Fujita, Y. (2008) *Photochem. Photobiol. Sci.*, 7: 1131-1149

2. Fujita Y, Bauer CE. (2003) The light-independent protochlorophyllide reductase: a nitrogenase-like enzyme catalyzing a key reaction for greening in the dark. In *Chlorophylls and Bilins: Biosynthesis, Synthesis, and Degradation*, ed. KM Kadish, KM Smith, R Guilard, pp. 109–56. New York: Academic Press.

3. Valera, V.; Fung,, M.; Wessler, A.N.; Richards, W.R. (1987) *Biochem. Biophys. Res. Commun.* 148: 515–520.

4. Begley, T.P.; Young, H. (1989) *J. Am. Chem. Soc.*, 111:3095-3096

5. Wilks, H.M. ;Timko, H.P. (1995) *Proc. Natl. Acad. Sci. USA*, 92:724-728

6 Heyes, D.J.; Heathcote, P.; Rigby, S.E.J.; Palacios, M.A.; van Grondelle, R.; Hunter, N.C. (2006) *J. Biol. Chem.*, 281:26847-26853

7 Heyes, D. J., Ruban, A. V., Wilks, H. M. and Hunter, C. N. (2002) *Proc. Natl. Acad. Sci. U.S.A.*, 99: 11145–11150

8 Heyes, D. J., Ruban, A. V. and Hunter, C. N. (2003) *Biochemistry*, 42: 523–528

9 Heyes, D. J. and Hunter, C. N. (2004) *Biochemistry*, 43: 8265–8271

10 Heyes, D.J.; Sakuma, M.; de Visser, S.P.; Scrutton, N.S. (2009) *J. Biol. Chem.*, 284:3762-3767

11 Becke, A. D. (1993) *J. Chem. Phys. I*, 98: 5648.

12 Lee, C.; Yang, W.; Parr, R. J. (1988) *Phys. Rev. B*, 37: 785.

13 Hertwig, R. W.; Koch, W. (1995) *J. Comp. Chem.*, 16: 576.

14 Baker, J., Kessi, A., Delley, B. (1996) *J.Chem.Phys.* 105: 192-212

15. Fernandes, P. A.; Ramos, M. J. (2004) *Chemistry,* 10: 257-266

16 Fernandes, P. A.; Ramos, M. J. (2003) *J. Am. Chem. Soc.*, 125: 6311-6322

17 Riley K.E., Op't Holt, B.T., Merz Jr., K.M. (2007) *J. Chem. Theory Comput.,* 3: 407-433

18 Townley, H.E., Sessions, R.B., Clarke, A.R., Dafforn, T.R. and Grifiths W.T. (2001) *Proteins*, 44: 329-335

19 Mulliken, R.S. *J. Chem. Phys.* (1995) 23: 1833

20 Lowdin, P.-O. (1970) *Adv. Chem. Phys.* 5: 185-199

21 A. A. Granovsky, PC GAMESS version 7.0, http://classic.chem.msu.su/gran/gamess/index.html

22 Schmidt, M.W., Baldridge, K.K., Boatz, J.A., Elbert, S.T., Gordon, M.S., Jensen, J.J., Koseki, S., Matsunaga, N., Nguyen, K.A., Su, S., Windus, T.L., Dupuis, M., Montgomery, J.A. (1993) *J.Comput.Chem.* 14: 1347-1363

23 Dreuw, A.; Weisman, J.L. and Head-Gordon, M. (2003), *J. Chem. Phys.*, 119: 2943-2946

24 Dreuw, A. and Head-Gordon, M. (2004), *J. Am. Chem. Soc.*, 126: 4007-4016

25 Starcke, J. H. ; Wormit, M.; Schirmer, J. and Dreuw, A. (2006) *Chem. Phys.*, 329: 39-49

26 Dreuw, A. and M. Head-Gordon (2005) *Chem. Rev.*, 105: 4009-4037

27 Kemble, E.C. (1937) "The Fundamental Principles of Quantum Mechanics with Elementary Applications", Dover Publications, New York.

28 Connor, J.N.L. (1968) *Mol. Phys.*, 15: 37-46

29 Marcus, R.A. (1965) *J. Chem. Phys.,* 43: 1598-1605

30 Miller, W.H. (1977) *Faraday Discuss. Chem. Soc.* 62: 40

31 Marcus, R.A. and Coltrin, M.E. (1977) *J. Phys. Chem.,* 67: 2609-2613

32 Garrett, B.C. and Truhlar, D. (1979) *J. Phys. Chem.,* 83: 2921-2926

33 Boys, S.F.; Bernardi, F. (1970) *Mol. Phys.*, 19: 553-566

34 Pu, J.; Gao, J.; Truhlar, D. G. (2006) *Chem. Rev.*,106: 3140-3169